ANTICANCER RESEARCH *41*: 2383-2395 (2021)
doi:10.21873/anticanres.15013

Modulation of Apoptosis and Epithelial-Mesenchymal Transition E-cadherin/TGF-β/Snail/TWIST Pathways by a New Ciprofloxacin Chalcone in Breast Cancer Cells

RANIA ALAAELDIN[1], GAMAL EL-DIN A. ABUO-RAHMA[2], QING-LI ZHAO[3] and MOUSTAFA FATHY[4,5]

[1]*Department of Biochemistry, Faculty of Pharmacy, Deraya University, Minia, Egypt;*
[2]*Department of Pharmaceutical Chemistry, Faculty of Pharmacy, Deraya University, Minia, Egypt;*
[3]*Department of Radiology, Graduate School of Medicine and Pharmaceutical Sciences, University of Toyama, Toyama, Japan;*
[4]*Department of Biochemistry, Faculty of Pharmacy, Minia University, Minia, Egypt;*
[5]*Department of Regenerative Medicine, Graduate School of Medicine and Pharmaceutical Sciences, University of Toyama, Toyama, Japan*

Abstract. *Background/Aim: This study aimed to investigate the effect of the new ciprofloxacin chalcone [7-(4-(N-substituted carbamoyl methyl) piperazin-1 yl)] on the proliferation, migration, and metastasis of MCF-7 and MDA-MB-231 breast cancer cell lines. Materials and Methods: Cell viability, colony formation and cell migration abilities were analysed. Cell cycle distribution and apoptosis were examined by flow cytometry. The molecular mechanism underlying chalcone's activity was investigated using qRT-PCR and western blotting. Results: This new ciprofloxacin chalcone significantly inhibited proliferation, colony formation, and cell migration abilities of both cancer cell lines. Furthermore, it initiated apoptosis and caused cell cycle arrest at G2/M and S phase in MCF-7 and MDA-MB-231 cell lines, respectively. In addition, it up-regulated the expression of pro-apoptotic factors, p53, PUMA and NOXA, and down-regulated the expression of anti-apoptotic factors, MDM2 and MDM4. At the same time, it inhibited epithelial–mesenchymal transition by increasing the expression of E-cadherin and decreasing the expression of TGF-β1, SNAI1, TWIST1, MMP2, and MMP9. Conclusion: This new ciprofloxacin chalcone exhibited promising apoptotic and anti-metastatic activities against MCF-7 and MDA-MB-231 breast cancer cell lines, and, therefore, is an attractive molecule for drug development in the treatment of breast cancer.*

Correspondence to: Qing-Li Zhao, Department of Radiology, Graduate School of Medicine and Pharmaceutical Sciences, University of Toyama, 2630 Sugitani, Toyama 930-0194, Japan. Tel: +81 764347267, Fax: +81 764345190, e-mail: zhao@med.u-toyama.ac.jp

Key Words: Breast cancer, ciprofloxacin chalcone, apoptosis, metastasis, epithelial–mesenchymal transition, P53, E-cadherin, TGF-β.

Breast cancer is the most common malignancy in women worldwide. Each year, approximately, 1.7 million new cases of breast cancer are diagnosed (1). Moreover, metastasis occurs in nearly 30% of breast cancer cases after treatment of the primary tumour (2). In addition, 90% of mortality is due to cancer invasion and metastasis (3). Thus, early detection of cancer (4, 5) and the identification of anti-cancer agents with promising anti-metastatic potential are important cancer therapy.

Cancer affects various pathways involved in angiogenesis and carcinogenesis (6-8). Many tumour suppressor genes are suppressed in the majority of cancers including *p53*, which is the main regulator of cellular responses to potentially oncogenic stimuli such as DNA damage, hypoxia, and metabolic stress (9). Mouse double minute 2 homolog (MDM2) and MDM4 play key roles in maintaining the normal activity of p53 in healthy normal cells, while their high expression contributes to inactivation of p53 (10). Therefore, MDM2 and MDM4 are considered potential targets for cancer therapy.

Screening existed agents for new therapeutic applications (11, 12) and alternative activities (13, 14) has become an attractive approach. One of the compounds that has shown alternative pharmacological activities is ciprofloxacin (15-17). Ciprofloxacin is a fourth-generation member of the fluoroquinolone family, which has an established safety profile as an antimicrobial agent for decades. It is very well known to target bacterial DNA replication and transcription through DNA topoisomerase II and gyrase (15). Furthermore, it has been thoroughly studied for its antiproliferative activity

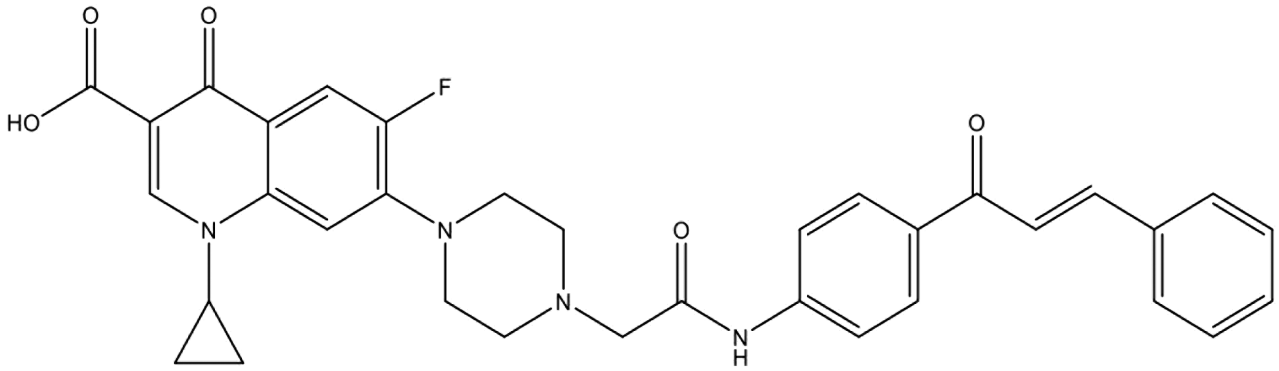

Figure 1. *Structure of the newly synthetized ciprofloxacin chalcone.*

against different cancer cells (16, 17). Numerous studies have suggested that structural modification may improve the potency and effectiveness of the parent drug (18). The C-7 position in the chemical structure of the parent drug has been the focus of many researchers reporting that it affects the mechanism of action, cell permeability as well as the pharmacokinetic properties of the drug (19). Additionally, the piperazine moiety at C-7 position showed structural flexibility to obtain new derivatives (19). Recent reports indicated that different derivatives of ciprofloxacin show potent cytotoxic activities (16, 20). Previously, we reported the anti-proliferative and apoptotic effect of a new ciprofloxacin-derivative against lung, colorectal, and cervical cancer cells (21, 22). As an extension of our previous findings, the main focus of this study was to investigate, for the first time, the effect of the new ciprofloxacin chalcone [7-(4-(N-substituted carbamoyl methyl) piperazin-1 yl)] on viability, proliferation, migration, and invasion abilities of breast cancer cell lines (MCF-7 and MDA-MB-231) and examine the molecular mechanism underlying this activity, aiming at identifying an attractive molecule for drug development in the treatment of breast cancer.

Materials and Methods

Synthesis of ciprofloxacin chalcone. The derivative was obtained in good yield following a reaction between the appropriate amine and bromoacetyl bromide utilizing potassium carbonate as a base in dichloromethane. Then alkylation of ciprofloxacin was performed with 2-bromoacetamide derivatives in acetonitrile in the presence of trimethylamine (TEA) (23, 24). This chalcone, shown in Figure 1, was identified and characterized by proton nuclear magnetic resonance (^{1}HNMR), carbon-13 NMR (^{13}C-NMR), and mass spectrometry as previously reported (24, 25).

Cell culture. MCF-7 and MDA-MB-231 cells were obtained from American type culture collection (ATCC, Manassas, VA, USA). Fresh Dulbecco's Modified Eagle's Medium (DMEM, Sigma-Aldrich, St Louis, MO, USA) was used as a culture medium, supplemented with 10% fetal bovine serum (FBS, Biosolutions International, Melbourne, Australia), 1% penicillin-streptomycin mixture (Invitrogen, Grand Island, NY, USA), and 1% L-glutamine (Sigma-Aldrich) in a humidified 5% CO_2 atmosphere at 37˚C.

Cell viability assay. Cell viability assay was achieved using the MTT reagent [3-(4, 5-dimethyl thiazol-2yl)-2, 5-diphenyltetrazolium bromide]. 10,000 MCF-7 and MDA-MB-231 cancer cells per well were seeded in triplicate in 96-well plates and allowed to grow in fresh DMEM medium for 24 h. Then, medium was changed with fresh DMEM containing different concentrations (20, 60, 180, 550, 1600 μM) of the tested chalcone. After incubation for 24 and 48 h, 10 μl of MTT (5 μg/ml) were added per well and incubated in the dark for 3 h at 37˚C. To dissolve the Formazan crystals that were formed, 100 μl of DMSO were used and absorbance was measured using an ELISA reader at 570 nM (26). The IC_{50} of the compound was calculated for each cell line using Graph Pad Prism-9 software.

Annexin V assay. Annexin V-FITC Apoptosis Detection Kit (Sigma-Aldrich) was used to detect apoptosis by flow cytometry, according to the manufacturer's instructions. Phosphatidyl serine sites on the cell membrane are marked with Annexin V-FITC. Propidium iodide (PI) marks the cellular DNA in necrotic cells. This combination allows discrimination between live cells (annexin V negative, PI negative), early apoptotic cells (annexin V positive, PI negative), late apoptotic (annexin V positive, PI positive), and necrotic cells (annexin V negative, PI positive). Using the IC_{50} of the tested chalcone (33.6±3.43 μM and 97.47±8.65 μM for MCF-7 and MDA-MB-231 cancer cells, respectively), the cancer cells were treated for 24 h. Then, untreated and treated cells were suspended in 1X Binding Buffer at a concentration of ~1×10^{6} cells/ml. Five μl of FITC-Conjugated Annexin V and 10 μl of propidium iodide solution were added in 500 μl of cell suspensions. The cells were incubated at room temperature for 10 min in the dark. Cell fluorescence was determined immediately with a flow cytometer (Becton Dickinson, Franklin Lakes, NJ, USA), by counting at least 10^{4} cells from each sample. Dot plots were obtained, and apoptosis was estimated.

Cell cycle analysis. For assessment of the cell cycle distribution, flow cytometric analysis using propidium iodide was performed in triplicate. A total of 1×10^{6} cells of both untreated and treated cancer

cells (treated for 24 h with the IC_{50} concentration of the examined chalcone, 33.6±3.43 μM and 97.47±8.65 μM for MCF-7 and MDA-MB-231 cancer cells, respectively) were collected by centrifugation, washed with phosphate buffer saline (PBS, pH=7.4, Sigma-Aldrich) and fixed with ice cold 66% ethanol. The fixed cells were washed with PBS and resuspended for 30 min in 1 mg/ml RNAse. Propidium iodide (50 μg/ml) was used to label the intracellular DNA by incubating the cells for at least 20 min at 4˚C in the dark. Then, samples were analysed using flow cytometry.

Colony formation assay. Cells were seeded in triplicate in 12-well plates at 500 cells/well and allowed to attach for 24 h in fresh DMEM medium. Then, the medium was changed to DMEM containing the IC_{50} of the examined chalcone, cells were incubated for 24 h, and doxorubicin was used as a positive control at the concentration of 1 μM (21, 25). Then, cells were washed with PBS twice and allowed to grow in fresh DMEM medium without the examined compound for 14 days at 37˚C in a humidified 5% CO_2 atmosphere, and the medium was changed twice a week. Then, cells were washed with PBS, fixed in 4% formaldehyde, and stained for 15 min with crystal violet. The number of colonies was estimated using the Image Processing and Analysis Java (ImageJ) program (National institutes of health, Bethesda, Maryland, United States). Colony formation ability was assessed by using the following equation:

$$\% \text{ of colony formation} = \frac{\text{no. of colonies}}{\text{no. of cells seeded}} * 100$$

Cell migration assay. Cells (1×10^6 cells) were seeded in triplicate in 35 mm cell culture dishes in DMEM medium and incubated at 37˚C in a humidified 5% CO_2 atmosphere for 24 h to attach. Then, a wound was created in the formed monolayers, using 200 μl tips. Cells were washed with PBS, treated with the IC_{50} of the examined chalcone in DMEM (33.6±3.43 μM and 97.47±8.65 μM for MCF-7 and MDA-MB-231 cancer cells, respectively), and incubated for 24 h. Doxorubicin was used as a positive control at the concentration of 1 μM. Images were captured using the cytosmart live-cell imaging system (Lonza Walkersville, Inc., Walkersville, MD, USA). Estimation of the open scratch area was performed at different time points using ImageJ, and data were analysed using GraphPad Prism-9 software (GraphPad, La Jolla, CA, USA).

RNA isolation and real-time qPCR assay. MCF-7 and MDA-MB-231 cancer cells were treated with the IC_{50} of the new chalcone, 33.6±3.43 μM and 97.47±8.65 μM, respectively, or 1 μM of doxorubicin, as a positive control (21, 25), for 24 h. Then, total RNA was extracted from the cells using the Qiagen RNA extraction kit (Hilden, Germany) according to the manufacturer's instructions. The expression of the *p53, MDM4, MDM2, p53 up-regulated modulator of apoptosis (PUMA), NOXA, E-cadherin, transforming growth factor (TGF-β1), SNAI1* and *Twist-related protein 1 (TWIST1)* genes was assessed by real-time qPCR. Quantification of mRNA was achieved by utilizing the Rotor-Gene 6000 Series Software 1.7 (Qiagen, Hilden, Germany). Glyceraldehyde 3-phosphate dehydrogenase (*GAPDH*) was used as internal control (27). The sequences of the primers are shown in Table I, and the primer sequences were obtained from National Centre for Biotechnology Information (NCBI). RT-PCR reactions, performed using the Qiagen one step RT-PCR (Qiagen) kit, contained 100 ng of total RNA, 1× buffer, 0.6 μM forward and reverse primers, 400 μM of each dNTP, and 2 μl enzyme mix. The conditions were as follows: 35 cycles of 25 s denaturation step at 95˚C, 30 s primer annealing at 58˚C, and 20 s polymerization at 72˚C.

Table I. *Primer sequences*.

Primer	Sequence of the primer
MDM4	Forward: 5'-TGTGGTGGAGATCTTTTGGG-3'
	Reverse: 5'-GCAGTGTGGGGATATCGT-3'.
MDM2	Forward: 5'-CGAGCGCCCAGTGCC-3'
	Reverse: 5'-AGGTGGTTACAGCACCATCAG-3'.
P53	Forward: 5'-GGTGACACGCTTCCCTGGAT-3'
	Reverse: 5'-CATCCATTGCTTGGGACGGC-3'.
PUMA	Forward: 5'-GTGGGTCCCCTGCCAGATT-3'
	Reverse: 5'-GGAGCTGCCCTCCTGGC-3'.
NOXA	Forward: 5'-CGAGGAACAAGTGCAAGTAGCTG-3'
	Reverse: 5'-GCCGGAAGTTCAGTTTGTCTCC-3'.
E-cadherin	Forward: 5'-ACTGATGCTGATGCCCCCAA-3'
	Reverse: 5'-TGTACTGCTGCTTGGCCTCA-3'
TGF-β1	Forward: 5'-CACCTTGGGCACTGTTGAAGT-3'
	Reverse: 5'-CCTCTCTGGGCTTGTTTCCTCA-3'
SNAI1	Forward: 5'-CGGCCTAGCGAGTGGTTCTT-3'
	Reverse: 5'-AGGAAAGAGCGCGGCATAGT-3'
TWIST1	Forward: 5'-ATGTCCGCGTCCCACTAGCA-3'
	Reverse: 5'-GCCCCACGCCCTGTTTCTTT-3'

Triplicate RT-PCR reactions were performed for each sample. Cycle threshold (Ct) was determined for each sample, and the average Ct was calculated. In order to exclude the production of non-specific DNA fragments and to characterize the obtained amplified mixture without the interference of contamination, a melting curve analysis was achieved between 60-95˚C at 1˚C intervals with the Rotor-Gene 6000 Series Software 1.7 (Qiagen), using the SYBR Green fluorescent dye. After normalization to the control *GAPDH* expression, the target gene expression in the treated cells relative to the untreated ones was calculated.

Analysis of protein expression via western blotting. To detect the expression levels of P53, MDM4, MDM2, Matrix metalloproteinase (MMP)-2 and MMP-9 proteins, sodium dodecyl sulphate–polyacrylamide gel electrophoresis (SDS-PAGE) analysis was performed. MCF-7 and MDA-MB-231 cells were treated with the IC_{50} of the chalcone, 33.6±3.43 μM and 97.47±8.65 μM, respectively, for 24 h or with 1 μM of doxorubicin, which was used as positive control. After washing with PBS, protein extraction was performed in RIPA lysis buffer, containing 50 mM Tris–Cl, pH 7.5, 0.1% SDS, 150 mM NaCl, 0.5% sodium deoxycholate, 1 mM PMSF, and 1% Nonidet P-40, supplemented with the complete protease inhibitor cocktail (Roche, Mannheim, Germany). The Bradford method was used to determine the protein concentration (28). Cell lysates containing 30 μg protein were separated by SDS-PAGE (15% acrylamide), transferred to a Hybond™ nylon membrane (GE Healthcare) and incubated for 1 h at room temperature in Blocking Solution. Membranes were incubated overnight at 4˚C with P53, MDM2, MDM4, MMP-2 and MMP-9 antibodies (New England Biolabs, Ipswich, MA, USA) diluted (1:1000) with PBS. Then,

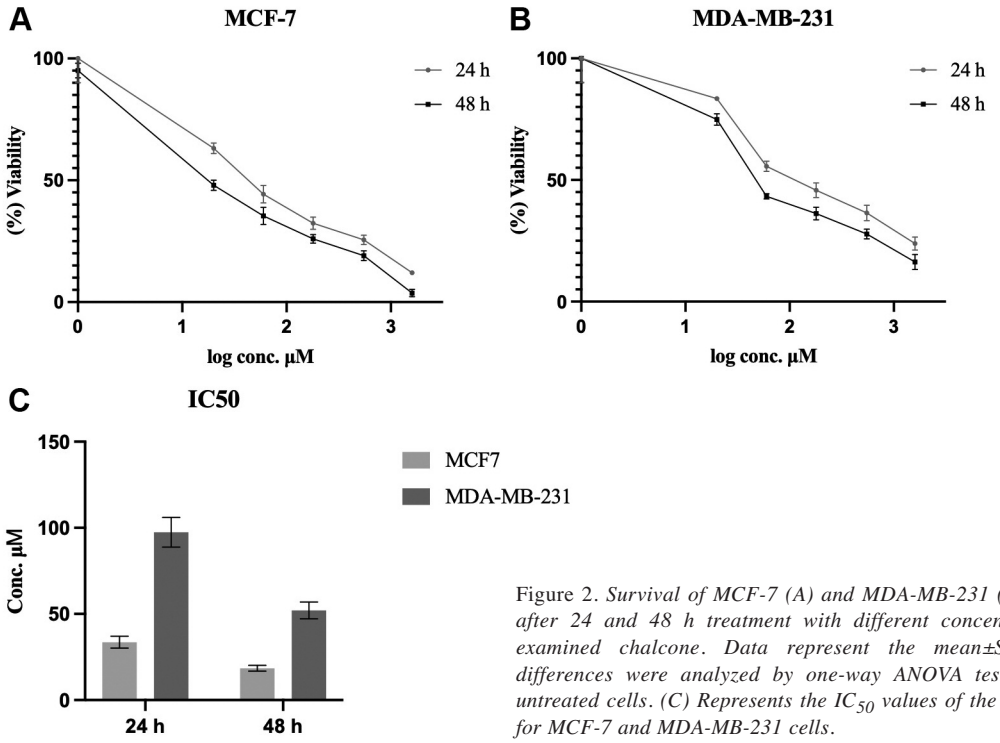

Figure 2. *Survival of MCF-7 (A) and MDA-MB-231 (B) cancer cells after 24 and 48 h treatment with different concentrations of the examined chalcone. Data represent the mean±SD. Significant differences were analyzed by one-way ANOVA test, compared to untreated cells. (C) Represents the IC_{50} values of the tested chalcone for MCF-7 and MDA-MB-231 cells.*

membranes were washed for 30-60 min and incubated at room temperature for 1 h with the HRP-conjugated secondary antibody (New England Biolabs) diluted (1:1000) in PBS (29). Immunoreactive proteins were detected using an enhanced chemiluminescence kit (GE Healthcare, Little Chalfont, UK) by a luminescent image analyzer (LAS-4000, Fujifilm Co., Tokyo, Japan). An antibody against β-actin (New England Biolabs) (1:1000) was used to detect β-actin, which was used as a loading control. Electrophoresis and electroblotting, using a discontinuous buffer system, were carried out in a Bio-Rad Trans-Blot SD Cell apparatus (Bio-Rad, Hercules, CA, USA). Densitometric analysis was then performed by using ImageJ. Data were normalized to β-actin levels.

Statistical analysis. Each experiment was repeated at least three times. Data are expressed as mean±standard deviation. Student's *t*-test was used to analyse differences after one-way analysis of variance (ANOVA), with the use of GraphPad Prism 9 statistical software (GraphPad) and Excel software (Microsoft, Redwood, WA, USA). Differences were considered significant when the probability values (p) were less than 0.05.

Results

Cell viability assay. The survival of MCF-7 and MDA-MB-231 cells was examined following treatment with different concentrations of the examined chalcone for 24 and 48 h. Survival of the cells was expressed as a percentage relative to that of the untreated cells, which was considered 100%. As shown in Figure 2A and B, the drug significantly inhibited the proliferation of both cell lines in a concentration- and time-dependent manner. The IC_{50} of the chalcone was 33.6±3.43 μM and 97.47±8.65 μM for MCF-7 and MDA-MB-231 after 24 h, respectively, whereas it was 18.48±1.73 μM and 52.10±4.87 μM for MCF-7 and MDA-MB-231 after 48 h, respectively, as shown in Figure 2C.

Annexin V assay using flow cytometry. Apoptotic cells were estimated using Annexin V assay. Cells were treated with the IC_{50} of the chalcone for 24 h. Apoptotic cells in the early phase (Annexin V-positive/PI-negative) can be distinguished from those in the late phase (Annexin V-positive/PI-positive) and necrotic phase (Annexin V-negative/PI-positive), as shown in Figure 3. The proportion of total apoptosis was significantly increased (p<0.001) from 0.66±0.03% to 12.71±1.37% and from 0.67±0.04% to 12.74±0.9% for MCF-7 and MDA-MB-231 cells, respectively, as shown in Figure 3E.

Cell cycle analysis using flow cytometry. To further determine the mechanism of apoptosis, we investigated the changes in cell cycle distribution after 24 h treatment with the IC_{50} of the chalcone in both cell lines. In accordance with the annexin V assay, the preG1 peak was significantly (p<0.001) increased in treated MCF-7 and MDA-MB-231 cells. Cell cycle arrest at the G_2/M and S phase for MCF-7 and MDA-MB-231 cells was observed, respectively (Figure 4).

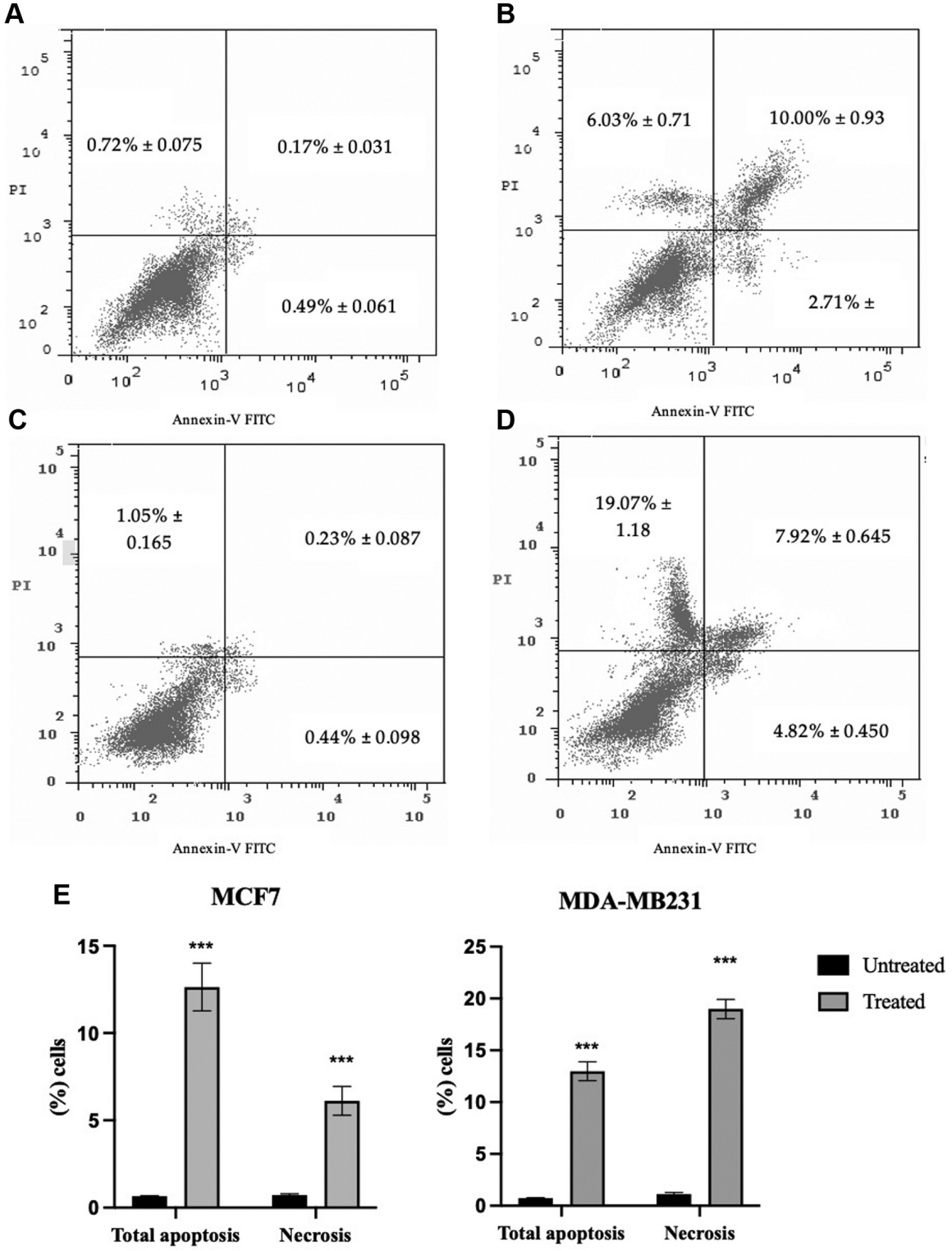

Figure 3. *Representative flow cytometric dot plots of Annexin V staining. (A) and (B) represent dot plots for untreated and treated MCF-7 cells, respectively. (C) and (D) represent dot plots for untreated and treated MDA-MB-231 cells, respectively. X axes and Y axes represent FITC-conjugated Annexin V and PE-conjugated PI, respectively. (E) The percentage of total apoptotic and necrotic cells in both cell lines after treatment with the* IC_{50} *of the chalcone for 24 h. Data represent the mean±SD. Significant difference was analyzed by one-way ANOVA test. ***p<0.0001 compared to untreated cells.*

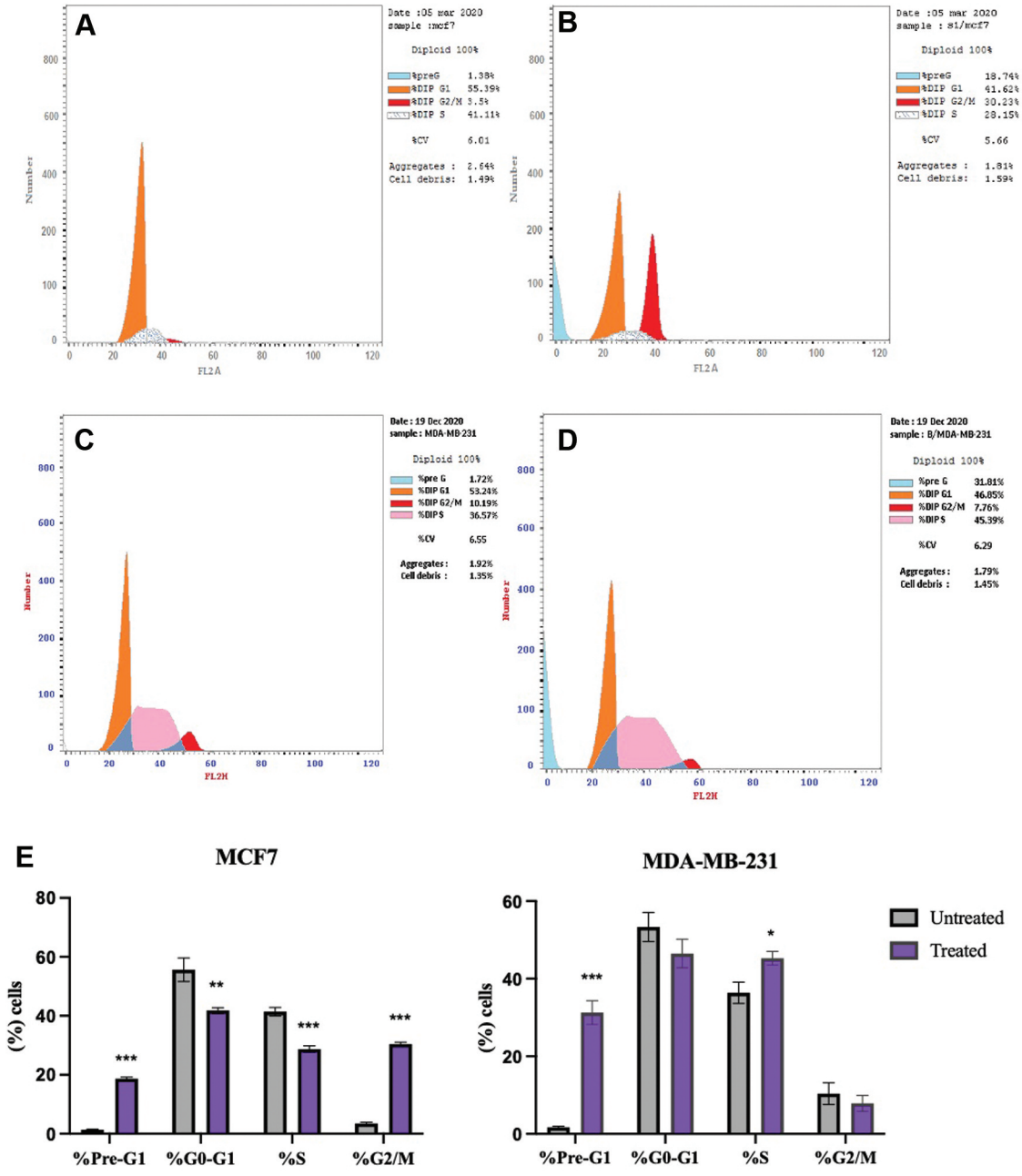

Figure 4. *Cell cycle phase distribution of untreated cells and cells treated with the IC_{50} concentration of the chalcone for 24 h as determined by flow cytometric analysis. (A) and (B) Representative histograms for cell cycle distribution after PI staining of untreated and treated MCF-7 cells, respectively. (C) and (D) Representative histograms for cell cycle distribution after PI staining of untreated and treated MDA-MB-231 cells, respectively. (E) Percentage of untreated and treated cells in the various cell cycle phases in both cell lines. Data represent the mean±SD. Significant difference was analyzed by one-way ANOVA test. *p<0.05, **p<0.01, ***p<0.001 compared to untreated cells.*

Colony formation assay. To examine the ability of the chalcone to inhibit colony formation from a single cell, a colony formation assay was performed after 24 h treatment with the IC_{50} of the tested chalcone. As shown in Figure 5, chalcone significantly (p<0.001) suppressed the ability of both cancer cells to form colonies. Doxorubicin was used as a positive control.

Cell migration assay. To investigate the migration inhibitory potential of the examined chalcone against breast cancer

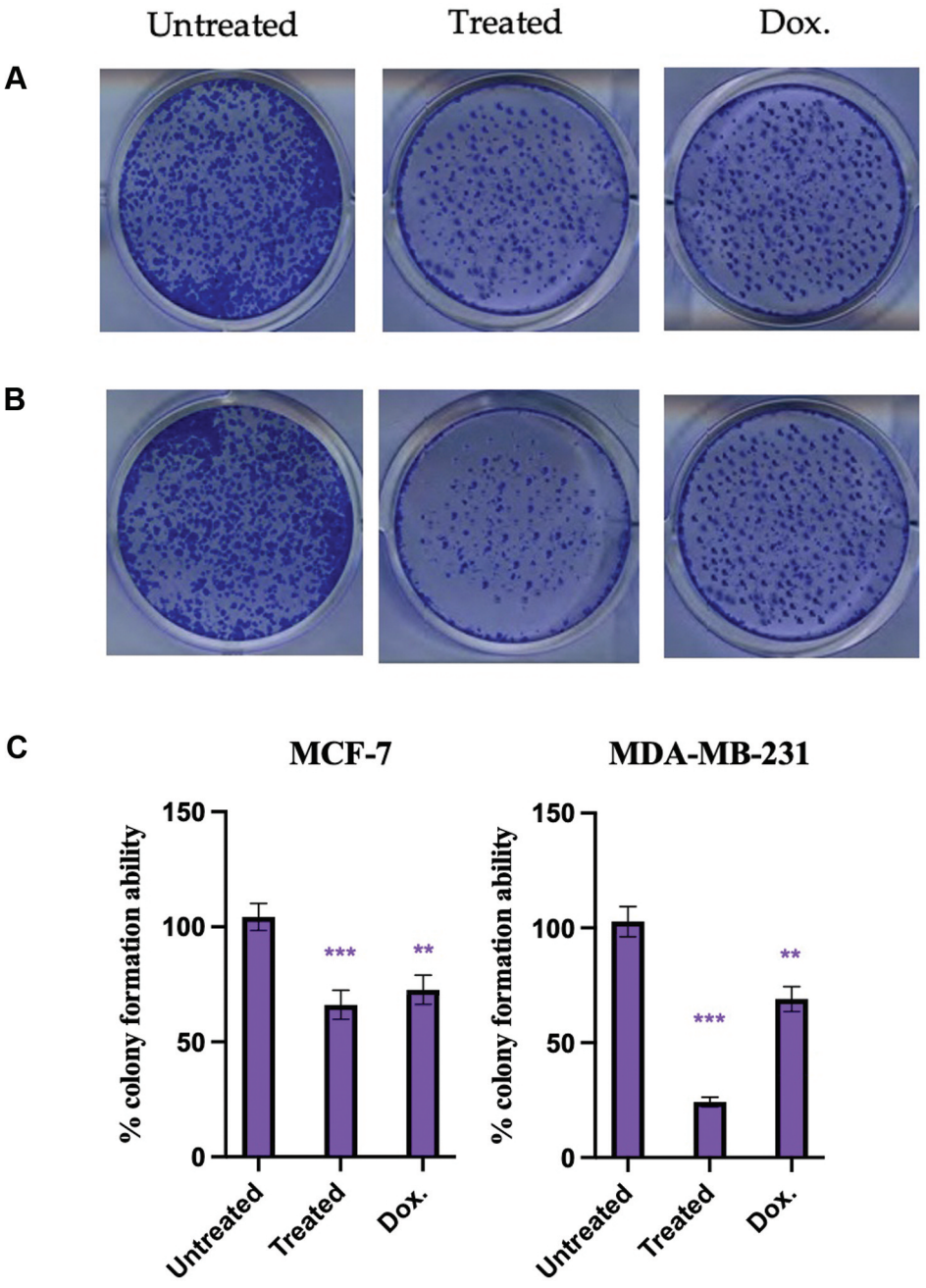

Figure 5. *Effect of the chalcone on colony formation. (A) and (B) colonies formed after treatment of MCF-7 and MDA-MB-231 cells with the* IC_{50} *of the chalcone, respectively. Doxorubicin was used as a positive control. (C) Graph showing the percentage of colony formation ability of both cell lines. Bars represent the mean±SD. **p<0.01, ***p<0.001 compared to untreated cells.*

cells, a cell migration assay was performed after 24 h treatment with the IC_{50} of the chalcone, as shown in Figure 6. The examined drug significantly ($p<0.05$) inhibited migration of MCF-7 cells where the percentage of wound closure was 68.34%±6.34, and potently ($p<0.01$) inhibited migration of MDA-MB-231 cells where the percentage of wound closure was 48.78%±4.67, as shown in Figure 6C. Doxorubicin was used as a positive control.

Expression of p53, MDM4, MDM2, PUMA, NOXA, E-cadherin, TGF-β1, SNAI1 and TWIST1 genes. The expression of the *p53, MDM4, MDM2, PUMA, NOXA, E-cadherin, TGF-*

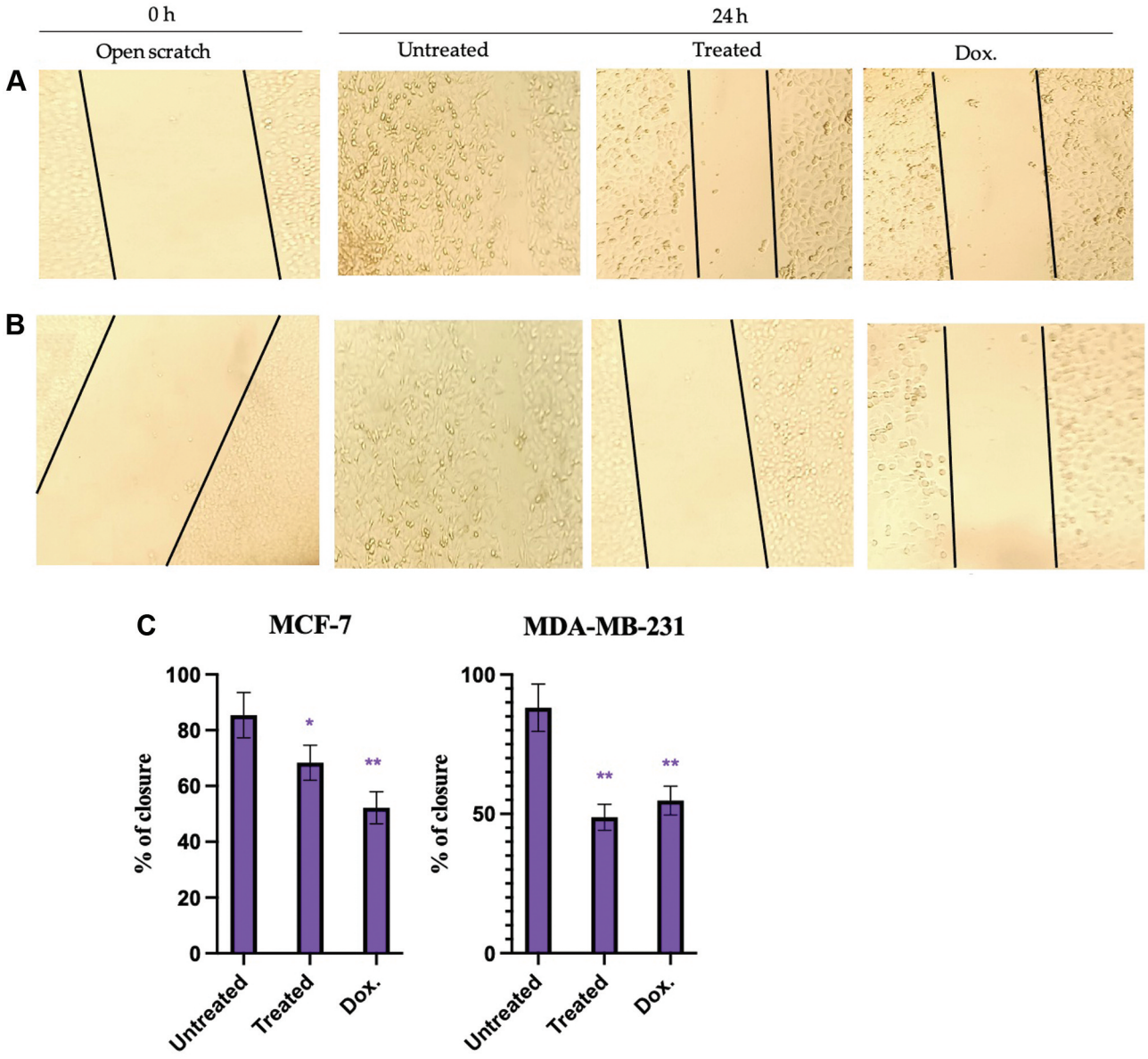

Figure 6. *Effect of the chalcone on the migration ability of cells. (A) and (B) Representative images were obtained at 0 and 24 h for untreated (control) and cells treated with the IC_{50} of the chalcone and doxorubicin following the generation of a scratch in MCF-7 and MDA-MB-231 cancer cells, respectively. Magnification: ×40. (C) Quantification of the percentage of closure by measuring the open scratch area at 0 and 24 h in MCF-7 and MDA-MB-231 cancer cells. *p<0.05, **p<0.01 compared to untreated cells.*

β1, SNAI1 and *TWIST1* genes was assessed by quantitative real time PCR (Figure 7). Gene expression was normalized to *GAPDH* and doxorubicin was used as a positive control. When compared to untreated cells, expression of *p53, PUMA, NOXA* and *E-cadherin* genes was significantly ($p<0.001$) increased in both cancer cells after treatment with the chalcone at the IC_{50} concentration for 24 h. Furthermore, the chalcone significantly ($p<0.001$) decreased the expression of *MDM4, MDM2, TGF-β1, SNAI1* and *TWIST1* genes.

Expression of P53, MDM4, MDM2, MMP-2 and MMP-9 proteins. Expression of P53, MDM4, MDM2, MMP-2 and MMP-9 proteins in MCF-7 and MDA-MB-231 cancer cells untreated or treated with the IC_{50} concentration of the chalcone for 24 h is shown in Figure 8A; doxorubicin was used as a positive control (Figure 8). Protein expression was normalized to β-actin protein. In chalcone-treated cells, when compared to untreated cells, expression of p53 protein was significantly ($p<0.001$) increased in MCF-7 and MDA-MB-

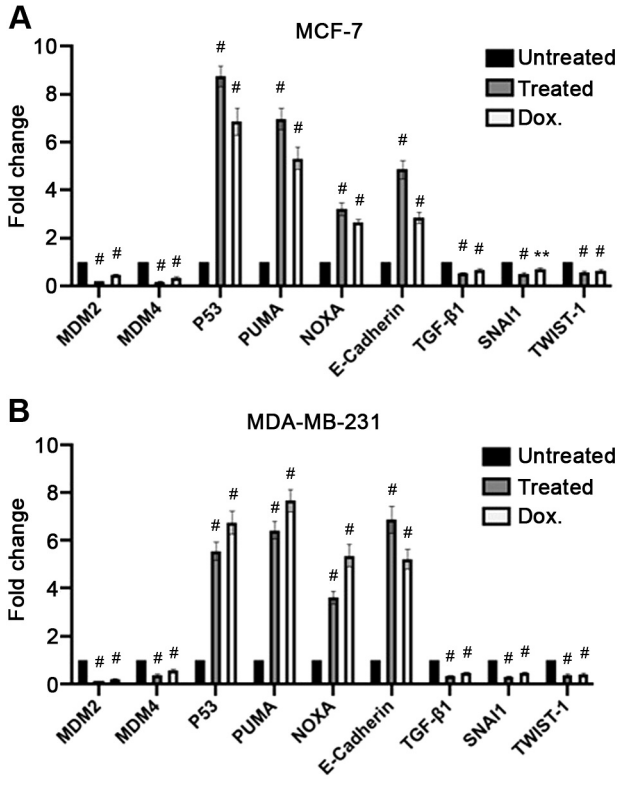

Figure 7. *Expression of p53, MDM4, MDM2, PUMA, NOXA, E-cadherin, TGF-β1, SNAI1 and TWIST1 genes was determined by quantitative real-time PCR. Relative gene expression in MCF-7 (A) and MDA-MB-231 (B) cells treated with the IC_{50} concentration of the chalcone for 24 h compared to untreated cells. Doxorubicin was used as a positive control. Expression was normalized to the corresponding GAPDH gene expression. Bars represent the mean±SD. Significant difference was analyzed by one-way ANOVA. **p<0.01, #p<0.001 compared to untreated cells.*

231 cancer cells. Whereas expression of MDM2, MDM4, MMP-2 and MMP-9 proteins was significantly (p<0.001) decreased in chalcone-treated MCF-7 and MDA-MB-231 cancer cells compared to untreated cells.

Discussion

Cancers are heterogenous, show differential resistance to the drugs and use different pathways to survive and grow (30-32). Therefore, continuous screening for new therapeutic agents with different pharmacological effects are required (33-37). Breast cancer is considered heterogenous at the clinical and molecular level, and is classified into many subtypes that have been identified through gene expression (38). Amongst recognized types, luminal A molecular subtype represents most of estrogen receptor (ER) and progesterone receptor (PR) positive malignancies, and accounts for 70% of breast cancer cases (39). Other subtypes of breast cancer include human epidermal growth factor receptor 2 (HER2)-positive cancer, which represents 15-20% of the cases and shows high levels of HER2 protein, and triple negative breast cancer (TNBC), which represents approximately 15% of all breast cancer cases and shows no expression of ER, PR, and HER2 proteins (40).

MCF-7 breast cancer cells are (ER)-positive and (PR)-positive (41), and belong to the luminal A molecular subtype (42). It is an appropriate model for different breast cancer studies especially those involving anticancer drugs. Despite the fact that luminal A molecular subtypes show sensitivity toward endocrine therapy, some possess or acquire resistance to treatment (43). Breast cancer patients with positive hormone receptor (HR+) status suffer from primary or secondary endocrine therapy resistance, which prevents effective treatment. MDA-MB-231 cells are from TNBC, and are characterized by the lack of ER, PR, and HER2 expression (44). TNBC is considered a highly aggressive tumour with great metastatic potential, high mortality rate, and poor clinical outcome (45). The molecular mechanisms of breast cancer genesis and progression are better understood nowadays (46), yet, the underlying mechanism of TNBC relapse has not been fully elucidated. Therefore, no targeted therapy has significantly improved patient survival (47). Moreover, traditional therapeutic strategies such as chemotherapy, radiation therapy, hormone therapy, and targeted therapy are still not adequate and usually accompanied by major side effects, including drug resistance, immune toxicity or unexpected toxicity (40). Therefore, finding new potential medications that target different pathways could help prevent or delay resistance to therapy.

In the present study, the effect of a new ciprofloxacin chalcone on the proliferation, migration, and invasion abilities of the breast cancer cell lines MCF-7 and MDA-MB-231, was investigated and the molecular mechanism underlying this activity was partially explained. The new chalcone inhibited proliferation and reduced viability of both cancer cell lines in a concentration-dependent manner, while the inhibition was more potent in MCF-7 cancer cells. Furthermore, annexin V staining and cell cycle analysis indicated that it induced apoptosis and cell cycle arrest. Specifically, our new ciprofloxacin chalcone induced cell cycle arrest at the G_2/M and S phases in MCF-7 and MDA-MB-231 cancer cells, respectively. This was further evidenced at the molecular level.

Inactivation of p53 in the majority of tumors may be due to genetic mutations or up-regulation of its inhibitory proteins such as MDM2 and MDM4, which target the transactivation domain of p53 and inhibit p53-mediated transcription. Furthermore, they trigger proteasomal degradation of p53 (48). Following treatment of MCF-7 and MDA-MB-231 cancer cells with the examined chalcone, the expression of MDM2

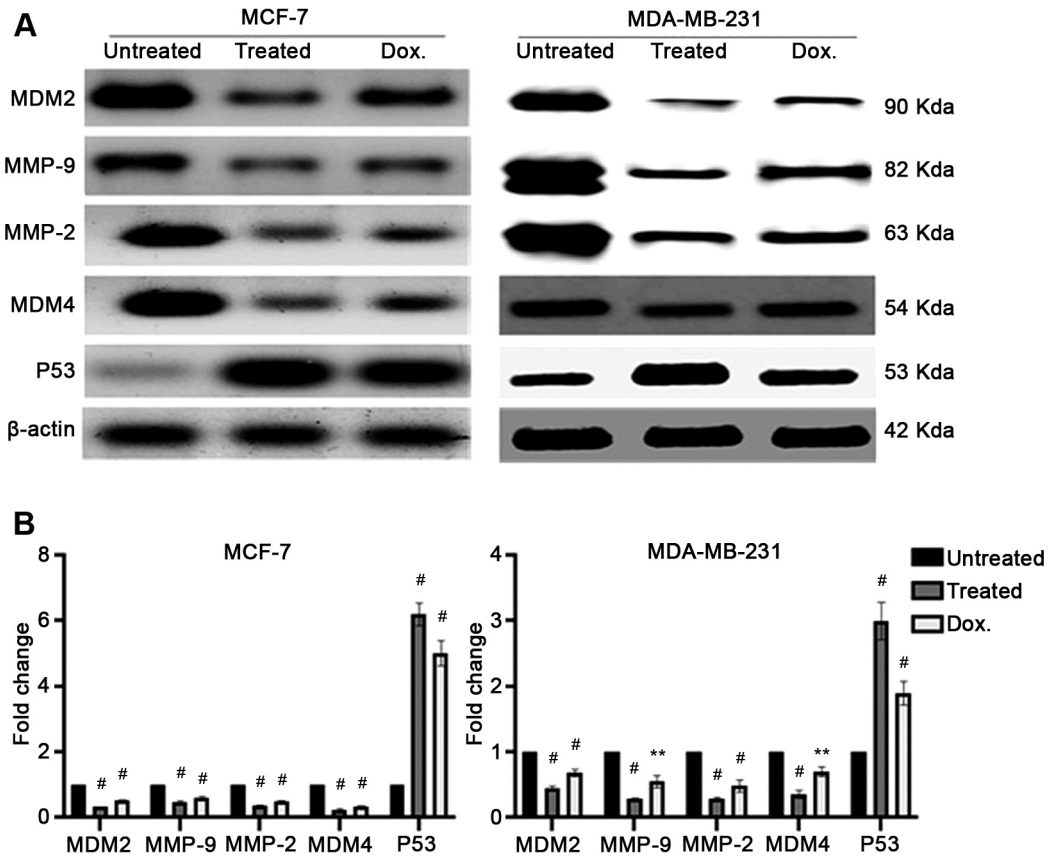

Figure 8. *Expression of P53, MDM4, MDM2, MMP 2 and MMP 9 proteins in MCF-7 and MDA-MB-231 cancer cells. (A) Representative western blots of P53, MDM4, MDM2, MMP-2 and MMP-9 proteins in MCF-7 and MDA-MB-231 cells treated with the IC_{50} concentration of the chalcone for 24 h. β-actin was used as an internal loading control and doxorubicin was used as a positive control. (B) Protein expression in MCF-7 and MDA-MB-231 treated cells relative to untreated cells after normalization to the corresponding β-actin protein levels. Bars represent the mean±SD. Significant difference was analyzed by one-way ANOVA, **p<0.01, #p<0.001, compared to untreated cells.*

and MDM4, on the gene and protein levels, was suppressed, whereas the expression of p53 was clearly increased. We hypothesize that the examined chalcone down-regulated the expression of MDM2 and MDM4 leading to the up-regulation of p53 expression, which is in accordance with Valianato *et al*. who suggested that other fluoroquinolone members could regulate specific miRNAs to cause alternative splicing on MDM4 transcript and interfere with its expression (49).

The up-regulation of p53 explains the induction of in both cancer cells. This was confirmed by the increase in the expression of pro-apoptotic genes, such as *PUMA* and *NOXA*. Once p53 expression is up-regulated, it activates pro-apoptotic BH-3 containing proteins, such as PUMA and NOXA, followed by binding with and inactivation of anti-apoptotic members of the bcl-2 family and further interaction with and activation of other pro-apoptotic proteins, such as Bak and Bax (50).

Importantly, in an attempt to investigate the anti-metastatic potential of the examined chalcone, colony formation and cell migration assays were performed. The results showed that chalcone suppressed the formation of colonies and migration abilities of both cells. Epithelial–mesenchymal transition (EMT) is critical for the conversion of primary localized tumors into invasive and metastatic cancers and is usually accompanied by chemoresistance and tumor stemness. The loss of cell adhesion and lack of epithelial properties in addition to gaining a mesenchymal phenotype are fundamental characteristics of an invasive capacity and migration (51). There are various pathways involved in EMT; the down-regulation of E-cadherin, a transmembrane molecule crucial for maintaining the epithelial phenotype and cell-cell interactions, is a hallmark of the EMT induction, which is accompanied by activation of different transcription factors such as Snail and Twist-1 that directly bind to the promoter region of E-cadherin and inhibit its transcription (52, 53). Another pathway for activating EMT is TGF-β/Smad signaling pathway. The

activation of this pathway results in the phosphorylation and activation of Smad2 and Smad3, which bind directly to the promoter region of Snail and activate its transcription leading to augmented down-regulation of E-cadherin expression (54). Matrix metalloproteinases (MMPs) are a family of calcium-containing and zinc-dependent proteases that facilitate the degradation of many extracellular matrix (ECM) proteins and basement membranes resulting in its remodeling, which is critical for cancer invasion and metastasis (55). MMP2 has been shown to degrade type IV, V, VI, and X collagens in addition to gelatins in the basement membranes, while MMP9 degrades type IV collagen and fibronectin in the basement membranes and ECM affecting the adhesion capacity of cancer cells. ECM and basement membranes are considered natural barriers against cancer cell migration, invasion, and metastasis (56).

Our findings are in accordance with the hypothesis that, in both breast cancer cell lines, EMT induction occurs *via* activation of many transcription factors including SNAI1 and Twist-1, along with the TGF-β pathway, which is accompanied by the down-regulation of E-cadherin and a high MMP2 and MMP9 expression. Our new ciprofloxacin chalcone significantly down-regulated the mRNA levels of Snail, Twist-1, and TGF-β along with the up-regulation of E-cadherin. Also, it inhibited the expression of MMP2 and MMP9 proteins in both breast cancer cell lines leading to significant suppression in their abilities for colony formation and cell migration, exhibiting promising anti-metastatic activity against both MCF-7 and MDA-MB-231 breast cancer cell lines.

In conclusion, the present study showed, for the first time, that this new ciprofloxacin chalcone [7-(4-(N-substituted carbamoyl methyl) piperazin-1yl)] targeted the p53/MDM2/MDM4/PUMA/NOXA pathway, which led to inhibition of proliferation and induced cell cycle arrest and apoptosis in MCF-7 and MDA-MB-231 cells. Furthermore, it inhibited their migration and metastatic ability by down-regulating MMP-2 and MMP-9 expression and inhibiting EMT through blocking the TGF-β pathway, suppressing SNAI1 and TWIST1 transcription factors, and increasing expression of E-cadherin. Therefore, this new ciprofloxacin chalcone exhibited promising apoptotic and anti-metastatic activities in MCF-7 and MDA-MB-231 breast cancer cell lines making it an attractive molecule for drug development in the treatment of breast cancer. Further studies of this new chalcone are required to increase our understanding of the molecular mechanisms underlying its effects.

Conflicts of Interest

The Authors declare no potential conflicts of interest regarding this study.

Authors' Contributions

Q.Z. and M.F. designed and supervised the research, evaluated the data and wrote the manuscript. R.A. was involved in data curation, formal analysis and writing–original draft of the manuscript. G.A. conceived the study and was involved in project administration. All Authors revised and approved the final article.

Acknowledgements

This work was supported in part by Japan Society for the Promotion of Science (JSPS) KAKENHI Grant Number JP18K07708.

References

1 Torre LA, Siegel RL, Ward EM and Jemal A: Global cancer incidence and mortality rates and trends – An update. Cancer Epidemiol Biomarkers Prev *25(1)*: 16-27, 2016. PMID: 26667886. DOI: 10.1158/1055-9965.EPI-15-0578

2 Balkwill FR, Capasso M and Hagemann T: The tumor microenvironment at a glance. J Cell Sci *125(Pt 23)*: 5591-5596, 2012. PMID: 23420197. DOI: 10.1242/jcs.116392

3 Sleeman J and Steeg PS: Cancer metastasis as a therapeutic target. Eur J Cancer *46(7)*: 1177-1180, 2010. PMID: 20307970. DOI: 10.1016/j.ejca.2010.02.039

4 Abd El-Baky RM, Hetta HF, Koneru G, Ammar M, Shafik EA, Mohareb DA, Abbas El-Masry M, Ramadan HK, Abu Rahma MZ, Fawzy MA and Fathy M: Impact of interleukin IL-6 rs-1474347 and IL-10 rs-1800896 genetic polymorphisms on the susceptibility of HCV-infected Egyptian patients to hepatocellular carcinoma. Immunol Res *68(3)*: 118-125, 2020. PMID: 32504406. DOI: 10.1007/s12026-020-09126-8

5 Abdel-hamid N, Ramadan M and Amgad S: Glycoregulatory enzymes as early diagnostic markers during premalignant stage in hepatocellular carcinoma. American Journal of Cancer Prevention *1(2)*: 14-19, 2013. DOI: 10.12691/ajcp-1-2-1

6 Fathy M, Khalifa EMMA and Fawzy MA: Modulation of inducible nitric oxide synthase pathway by eugenol and telmisartan in carbon tetrachloride-induced liver injury in rats. Life Sci *216*: 207-214, 2019. PMID: 30452970. DOI: 10.1016/j.lfs.2018.11.031

7 Fathy M and Nikaido T: *In vivo* modulation of iNOS pathway in hepatocellular carcinoma by Nigella sativa. Environ Health Prev Med *18(5)*: 377-385, 2013. PMID: 23609474. DOI: 10.1007/s12199-013-0336-8

8 Fathy M and Nikaido T: *In vivo* attenuation of angiogenesis in hepatocellular carcinoma by Nigella sativa. Turk J Med Sci *48(1)*: 178-186, 2018. PMID: 29479981. DOI: 10.3906/sag-1701-86

9 Vousden KH and Lane DP: p53 in health and disease. Nat Rev Mol Cell Biol *8(4)*: 275-283, 2007. PMID: 17380161. DOI: 10.1038/nrm2147

10 Toledo F and Wahl GM: Regulating the p53 pathway: *In vitro* hypotheses, *in vivo* veritas. Nat Rev Cancer *6(12)*: 909-923, 2006. PMID: 17128209. DOI: 10.1038/nrc2012

11 Fathy M, Fawzy MA, Hintzsche H, Nikaido T, Dandekar T and Othman EM: Eugenol exerts apoptotic effect and modulates the sensitivity of HeLa cells to cisplatin and radiation. Molecules *24(21)*:3979, 2019. PMID: 31684176. DOI: 10.3390/molecules 24213979

12 Fathy M, Okabe M, Saad Eldien HM and Yoshida T: AT-MSCs antifibrotic activity is improved by eugenol through modulation of TGF-β/Smad signaling pathway in rats. Molecules *25(2)*:348, 2020. PMID: 31952158. DOI: 10.3390/molecules25020348

13 Oba J, Okabe M, Yoshida T, Soko C, Fathy M, Amano K, Kobashi D, Wakasugi M and Okudera H: Hyperdry human amniotic membrane application as a wound dressing for a full-thickness skin excision after a third-degree burn injury. Burns Trauma *8*: tkaa014, 2020. PMID: 32733973. DOI: 10.1093/burnst/tkaa014

14 Otaka S, Nagura S, Koike C, Okabe M, Yoshida T, Fathy M, Yanagi K, Misaki T and Nikaido T: Selective isolation of nanog-positive human amniotic mesenchymal cells and differentiation into cardiomyocytes. Cell Reprogram *15(1)*: 80-91, 2013. PMID: 23298400. DOI: 10.1089/cell.2012.0028

15 Zhao X, Xu C, Domagala J and Drlica K: DNA topoisomerase targets of the fluoroquinolones: A strategy for avoiding bacterial resistance. Proc Natl Acad Sci USA *94(25)*: 13991-13996, 1997. PMID: 9391140. DOI: 10.1073/pnas.94.25.13991

16 Kassab AE and Gedawy EM: Novel ciprofloxacin hybrids using biology oriented drug synthesis (BIODS) approach: Anticancer activity, effects on cell cycle profile, caspase-3 mediated apoptosis, topoisomerase II inhibition, and antibacterial activity. Eur J Med Chem *150*: 403-418, 2018. PMID: 29547830. DOI: 10.1016/j.ejmech.2018.03.026

17 Sedghizadeh PP, Sun S, Junka AF, Richard E, Sadrerafi K, Mahabady S, Bakhshalian N, Tjokro N, Bartoszewicz M, Oleksy M, Szymczyk P, Lundy MW, Neighbors JD, Russell RG, McKenna CE and Ebetino FH: Design, synthesis, and antimicrobial evaluation of a novel bone-targeting bisphosphonate-ciprofloxacin conjugate for the treatment of osteomyelitis biofilms. J Med Chem *60(6)*: 2326-2343, 2017. PMID: 28121436. DOI: 10.1021/acs.jmedchem.6b01615

18 Buglak AA, Shanin IA, Eremin SA, Lei HT, Li X, Zherdev AV and Dzantiev BB: Ciprofloxacin and clinafloxacin antibodies for an immunoassay of quinolones: Quantitative structure-activity analysis of cross-reactivities. Int J Mol Sci *20(2)*:265, 2019. PMID: 30641870. DOI: 10.3390/ijms20020265

19 Esfahani E, Mohammadi-khanaposhtani M, Rezaei Z, Valizadeh Y, Rajabnia R, Hassankalhori M, Bandarian F, Faramarzi M, Samadi N, Amini M, Mahdavi M and Larijani B: New ciprofloxacin–dithiocarbamate–benzyl hybrids: Design, synthesis, antibacterial evaluation, and molecular modeling studies. Research on Chemical Intermediates *45(2)*: 223-236, 2019. DOI: 10.1007/s11164-018-3598-3

20 Chrzanowska A, Roszkowski P, Bielenica A, Olejarz W, Stępień K and Struga M: Anticancer and antimicrobial effects of novel ciprofloxacin fatty acids conjugates. Eur J Med Chem *185*: 111810, 2020. PMID: 31678743. DOI: 10.1016/j.ejmech.2019.111810

21 Alaaeldin R, Nazmy MH, Abdel-Aziz M, Abuo-Rahma GEA and Fathy M: Cell cycle arrest and apoptotic effect of 7-(4-(N-substituted carbamoylmethyl) piperazin-1-yl) ciprofloxacin-derivative on HCT 116 and A549 cancer cells. Anticancer Res *40(5)*: 2739-2749, 2020. PMID: 32366419. DOI: 10.21873/anticanres.14245

22 Fathy M, Sun S, Zhao QL, Abdel-Aziz M, Abuo-Rahma GEA, Awale S and Nikaido T: A new ciprofloxacin-derivative inhibits proliferation and suppresses the migration ability of HeLa cells. Anticancer Res *40(9)*: 5025-5033, 2020. PMID: 32878790. DOI: 10.21873/anticanres.14505

23 Yadav V, Varshney P, Sultana S, Yadav J and Saini N: Moxifloxacin and ciprofloxacin induces S-phase arrest and augments apoptotic effects of cisplatin in human pancreatic cancer cells *via* ERK activation. BMC Cancer *15*: 581, 2015. PMID: 26260159. DOI: 10.1186/s12885-015-1560-y

24 Abdel-Aziz AA, El-Azab AS, Alanazi AM, Asiri YA, Al-Suwaidan IA, Maarouf AR, Ayyad RR and Shawer TZ: Synthesis and potential antitumor activity of 7-(4-substituted piperazin-1-yl)-4-oxoquinolines based on ciprofloxacin and norfloxacin scaffolds: *In silico* studies. J Enzyme Inhib Med Chem *31(5)*: 796-809, 2016. PMID: 26226179. DOI: 10.3109/14756366.2015.1069288

25 Mohammed HHH, Abd El-Hafeez AA, Abbas SH, Abdelhafez EMN and Abuo-Rahma GEA: New antiproliferative 7-(4-(N-substituted carbamoylmethyl)piperazin-1-yl) derivatives of ciprofloxacin induce cell cycle arrest at G2/M phase. Bioorg Med Chem *24(19)*: 4636-4646, 2016. PMID: 27555286. DOI: 10.1016/j.bmc.2016.07.070

26 Goel A, Prasad AK, Parmar VS, Ghosh B and Saini N: Apoptogenic effect of 7,8-diacetoxy-4-methylcoumarin and 7,8-diacetoxy-4-methylthiocoumarin in human lung adenocarcinoma cell line: role of NF-kappaB, Akt, ROS and MAP kinase pathway. Chem Biol Interact *179(2-3)*: 363-374, 2009. PMID: 19061872. DOI: 10.1016/j.cbi.2008.10.060

27 Barber RD, Harmer DW, Coleman RA and Clark BJ: GAPDH as a housekeeping gene: Analysis of GAPDH mRNA expression in a panel of 72 human tissues. Physiol Genomics *21(3)*: 389-395, 2005. PMID: 15769908. DOI: 10.1152/physiolgenomics.00025.2005

28 Bradford MM: A rapid and sensitive method for the quantitation of microgram quantities of protein utilizing the principle of protein-dye binding. Anal Biochem *72*: 248-254, 1976. PMID: 942051. DOI: 10.1006/abio.1976.9999

29 Greenfield EA: Antibodies: A laboratory manual. Cold Spring Harbor Laboratory Press, 2013.

30 Fathy M, Awale S and Nikaido T: Phosphorylated Akt protein at Ser473 enables HeLa cells to tolerate nutrient-deprived conditions. Asian Pac J Cancer Prev *18(12)*: 3255-3260, 2017. PMID: 29286216. DOI: 10.22034/APJCP.2017.18.12.3255

31 Noto Z, Yoshida T, Okabe M, Koike C, Fathy M, Tsuno H, Tomihara K, Arai N, Noguchi M and Nikaido T: CD44 and SSEA-4 positive cells in an oral cancer cell line HSC-4 possess cancer stem-like cell characteristics. Oral Oncol *49(8)*: 787-795, 2013. PMID: 23768762. DOI: 10.1016/j.oraloncology.2013.04.012

32 Wang F, Yoshida T, Okabe M, Fathy M, Sun Y, Koike C, Saito S and Nikaido T: CD24+SSEA4+cells in ovarian carcinoma cells demonstrated the characteristics as cancer stem cells. Journal of Cancer Science & Therapy *09(03)*: 2017. DOI: 10.4172/1948-5956.1000440

33 Fathy M, Okabe M, M Othman E, Saad Eldien HM and Yoshida T: Preconditioning of adipose-derived mesenchymal stem-like cells with eugenol potentiates their migration and proliferation *in vitro* and therapeutic abilities in rat hepatic fibrosis. Molecules *25(9)*: 2020, 2020. PMID: 32357508. DOI: 10.3390/molecules25092020

34 Nagura S, Otaka S, Koike C, Okabe M, Yoshida T, Fathy M, Fukahara K, Yoshimura N, Misaki T and Nikaido T: Effect of exogenous Oct4 overexpression on cardiomyocyte differentiation of human amniotic mesenchymal cells. Cell Reprogram *15(5)*: 471-480, 2013. PMID: 24073944. DOI: 10.1089/cell.2013.0002

35 Naseem M, Othman EM, Fathy M, Iqbal J, Howari FM, AlRemeithi FA, Kodandaraman G, Stopper H, Bencurova E, Vlachakis D and Dandekar T: Integrated structural and functional analysis of the protective effects of kinetin against oxidative stress in mammalian cellular systems. Sci Rep *10(1)*: 13330, 2020. PMID: 32770053. DOI: 10.1038/s41598-020-70253-1

36 Okabe M, Yoshida T, Suzuki M, Goto M, Omori M, Taguchi M, Toda A, Suzuki T, Nakagawa K, Hiramoto F, Ushijima T, Waki H, Furuichi E, Arai K, Zhou K, Fathy omar M, Nakamura M, Nomura Y, Kasama T, Katou K, Saito S and Nikaido T: Hyperdry human amniotic membrane (HD-AM) is supporting aciclovir included device of Poly-N-p-Vinyl-Benzyl-D-Lactonamide (PVLA) sphere for treatment of HSV-1 infected rabbit Keratitis model. Journal of Biotechnology & Biomaterials *07(01)*: 2017. DOI: 10.4172/2155-952X.1000251

37 Othman EM, Fathy M, Bekhit AA, Abdel-Razik AH, Jamal A, Nazzal Y, Shams S, Dandekar T and Naseem M: Modulatory and toxicological perspectives on the effects of the small molecule kinetin. Molecules *26(3)*: 670, 2021. PMID: 33525350. DOI: 10.3390/molecules26030670

38 Curtis C, Shah SP, Chin SF, Turashvili G, Rueda OM, Dunning MJ, Speed D, Lynch AG, Samarajiwa S, Yuan Y, Gräf S, Ha G, Haffari G, Bashashati A, Russell R, McKinney S, METABRIC Group., Langerød A, Green A, Provenzano E, Wishart G, Pinder S, Watson P, Markowetz F, Murphy L, Ellis I, Purushotham A, Børresen-Dale AL, Brenton JD, Tavaré S, Caldas C and Aparicio S: The genomic and transcriptomic architecture of 2,000 breast tumours reveals novel subgroups. Nature *486(7403)*: 346-352, 2012. PMID: 22522925. DOI: 10.1038/nature10983

39 Ciriello G, Sinha R, Hoadley KA, Jacobsen AS, Reva B, Perou CM, Sander C and Schultz N: The molecular diversity of Luminal A breast tumors. Breast Cancer Res Treat *141(3)*: 409-420, 2013. PMID: 24096568. DOI: 10.1007/s10549-013-2699-3

40 Eiro N, Gonzalez LO, Fraile M, Cid S, Schneider J and Vizoso FJ: Breast cancer tumor stroma: Cellular components, phenotypic heterogeneity, intercellular communication, prognostic implications and therapeutic opportunities. Cancers (Basel) *11(5)*: 664, 2019. PMID: 31086100. DOI: 10.3390/cancers11050664

41 Comşa Ş, Cîmpean AM and Raica M: The story of MCF-7 breast cancer cell line: 40 years of experience in research. Anticancer Res *35(6)*: 3147-3154, 2015. PMID: 26026074.

42 Kang Y and Kim SD: 11th international conference on gas-liquid and gas-liquid-solid reactor engineering (gls-11) preface. Chem Eng Sci 100: 1-1, 2013. DOI: 10.1016/j.ces.2013.06.040

43 Ring A and Dowsett M: Mechanisms of tamoxifen resistance. Endocr Relat Cancer *11(4)*: 643-658, 2004. PMID: 15613444. DOI: 10.1677/erc.1.00776

44 Brown M, Tsodikov A, Bauer KR, Parise CA and Caggiano V: The role of human epidermal growth factor receptor 2 in the survival of women with estrogen and progesterone receptor-negative, invasive breast cancer: The California Cancer Registry, 1999-2004. Cancer *112(4)*: 737-747, 2008. PMID: 18189290. DOI: 10.1002/cncr.23243

45 Dent R, Trudeau M, Pritchard KI, Hanna WM, Kahn HK, Sawka CA, Lickley LA, Rawlinson E, Sun P and Narod SA: Triple-negative breast cancer: Clinical features and patterns of recurrence. Clin Cancer Res *13(15 Pt 1)*: 4429-4434, 2007. PMID: 17671126. DOI: 10.1158/1078-0432.CCR-06-3045

46 Anderberg C and Pietras K: On the origin of cancer-associated fibroblasts. Cell Cycle *8(10)*: 1461-1462, 2009. PMID: 19395855. DOI: 10.4161/cc.8.10.8557

47 Garrido-Castro AC, Lin NU and Polyak K: Insights into molecular classifications of triple-negative breast cancer: Improving patient selection for treatment. Cancer Discov *9(2)*: 176-198, 2019. PMID: 30679171. DOI: 10.1158/2159-8290.CD-18-1177

48 Wade M, Li YC and Wahl GM: MDM2, MDMX and p53 in oncogenesis and cancer therapy. Nat Rev Cancer *13(2)*: 83-96, 2013. PMID: 23303139. DOI: 10.1038/nrc3430

49 Valianatos G, Valcikova B, Growkova K, Verlande A, Mlcochova J, Radova L, Stetkova M, Vyhnakova M, Slaby O and Uldrijan S: A small molecule drug promoting miRNA processing induces alternative splicing of MdmX transcript and rescues p53 activity in human cancer cells overexpressing MdmX protein. PLoS One *12(10)*: e0185801, 2017. PMID: 28973015. DOI: 10.1371/journal.pone.0185801

50 Zhang LN, Li JY and Xu W: A review of the role of Puma, Noxa and Bim in the tumorigenesis, therapy and drug resistance of chronic lymphocytic leukemia. Cancer Gene Ther *20(1)*: 1-7, 2013. PMID: 23175245. DOI: 10.1038/cgt.2012.84

51 Krantz SB, Shields MA, Dangi-Garimella S, Munshi HG and Bentrem DJ: Contribution of epithelial-to-mesenchymal transition and cancer stem cells to pancreatic cancer progression. J Surg Res *173(1)*: 105-112, 2012. PMID: 22099597. DOI: 10.1016/j.jss.2011.09.020

52 Onder TT, Gupta PB, Mani SA, Yang J, Lander ES and Weinberg RA: Loss of E-cadherin promotes metastasis *via* multiple downstream transcriptional pathways. Cancer Res *68(10)*: 3645-3654, 2008. PMID: 18483246. DOI: 10.1158/0008-5472.CAN-07-2938

53 Higuchi O, Okabe M, Yoshida T, Fathy M, Saito S, Miyawaki T and Nikaido T: Stemness of human Wharton's jelly mesenchymal cells is maintained by floating cultivation. Cell Reprogram *14(5)*: 448-455, 2012. PMID: 22908943. DOI: 10.1089/cell.2012.0020

54 Ioannou M, Kouvaras E, Papamichali R, Samara M, Chiotoglou I and Koukoulis G: Smad4 and epithelial-mesenchymal transition proteins in colorectal carcinoma: An immunohistochemical study. J Mol Histol *49(3)*: 235-244, 2018. PMID: 29468299. DOI: 10.1007/s10735-018-9763-6

55 Lai YH, Chen J, Wang XP, Wu YQ, Peng HT, Lin XH and Wang WJ: Collagen triple helix repeat containing-1 negatively regulated by microRNA-30c promotes cell proliferation and metastasis and indicates poor prognosis in breast cancer. J Exp Clin Cancer Res *36(1)*: 92, 2017. PMID: 28697793. DOI: 10.1186/s13046-017-0564-7

56 Li H, Huang J, Yang B, Xiang T, Yin X, Peng W, Cheng W, Wan J, Luo F, Li H and Ren G: Mangiferin exerts antitumor activity in breast cancer cells by regulating matrix metalloproteinases, epithelial to mesenchymal transition, and β-catenin signaling pathway. Toxicol Appl Pharmacol *272(1)*: 180-190, 2013. PMID: 23707762. DOI: 10.1016/j.taap.2013.05.011

Received March 11, 2021
Revised March 30, 2021
Accepted April 1, 2021